# SUPPORTING INFORMATION

Reaction Mechanism and Kinetics for Carbon Dioxide Reduction on Iron-Nickel Bi-Atom Catalysts

Fuhua Li, Huaqiang Wen and Qing Tang*

School of Chemistry and Chemical Engineering, Chongqing Key Laboratory of Theoretical and Computational Chemistry, Chongqing University, Chongqing 401331, China

*To whom correspondence should be addressed. E-mail: qingtang@cqu.edu.cn.

Grand canonical potential kinetics formulation. Different from the traditional Butler-Volmer description of electrochemical process, the GCP-K method enables the U to be fixed as its initial state via tuning the charges of system to hold fractional occupations. The schematic principles and difference between Butler-Volmer method and GCP-K is depicted as **Scheme S1**. Particularly, the calculation of electron number- and voltage-dependent grand canonical potential, $G(n; U)$, can be easily achieved by firstly calculating fixed-electron free energy, $F(n)$, and then converting $F(n)$ to grand canonical potential $G(U)$ via Legendre transformation.[1-3]

(a) Butler-Volmer kinetics
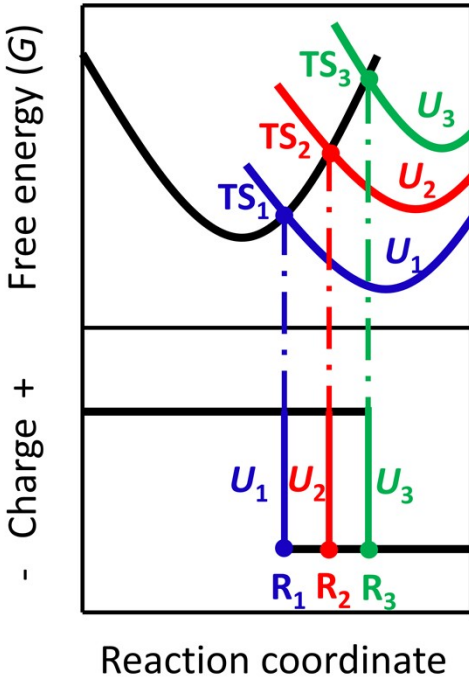
(b) GCP kinetics
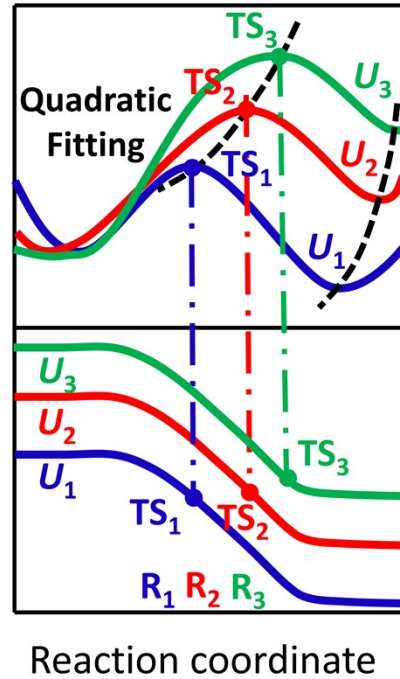
Scheme S1. The voltage depended electrochemical process described by (a) Butler-Volmer kinetics and by (b) grand canonical potential kinetics (GCP-K). Of note the Butler-Volmer description could be seen as a special case of the GCP-K scheme that the electron transfer occurs instantaneously.

Common quantum mechanics methods, e.g. DFT calculations, are usually carried out with fixed number of electrons. The methodological modification is hence necessary to coincide the calculation with realistic electrochemical process under a specified applied voltage. One way is to construct the relation between the electron numbers and the work function of the slab interface, which usually includes the effect of uniform background charge,[4-6] explicit ions,[4, 5] and surface coverage[7] of adsorbate. Another way is to belong the counter-ions to implicit solvation and integrate the solvation and interface as a slab-solvent combination system, and the corresponding grand canonical potential G(n; U) is obtained with the following formula 1.[8, 9]

$$G(n;U) = F(n) - ne(U_{\text{SHE}} - U) \tag{1}$$

Where U is the applied potential (used in experiment, U vs SHE), U_{SHE} represents the electronic energy in standard hydrogen electrode environment (SHE, $U_{\text{SHE}} = \mu_{e,\text{SHE}/e}$). Note that the relation "$G(n;U) = F(n) - n\mu_e = F(n) - ne(U_{SHE} - U)$" rationally describes the thermodynamic basis of the electrochemical grand canonical formulation "$\Omega \equiv A - \mu_e N_e$", on the condition that (1) the Helmholtz free energy A can be estimated with high accuracy by the ab initio electrochemical modeling, and (2) the theoretical absolute U_{SHE} is accurately calibrated from theoretical PZC vs experimental PZC (vs. SHE) such that the electron chemical potential μ_e can be absolutely converted to an electrode potential U relative to U_{SHE} ($\mu_e = e(U_{SHE} - U)$, $U_{SHE} = 4.66V$). From the $G(n;U)$ definition, only the difference between G values of two states/species is meaningful because the reference state for the free energy is arbitrary. In order to depict the relation of electron number and the applied potential and further obtain G(n; U) as the thermodynamic potential, the electron number of the system is artificially varied for tuning the electronic band occupation and further matching the Fermi level to the corresponding applied potentials, as the equation 2.[10, 11] Then the macroscopic thermodynamic GCP(U) can be defined and obtained by minimizing G(n; U) according to equation 3.[12, 13]

$$\frac{\mathrm{d}G(n;U)}{\mathrm{d}n} = 0 \text{ or } \mu_e = \frac{\mathrm{d}F(n)}{\mathrm{d}n} = e(U_{\text{SHE}} - U) \tag{2}$$

$$\text{GCP}(U) = \min_{n} G(n;U) = \min_{n} [F(n) - ne(U_{\text{SHE}} - U)] \tag{3}$$

Because the experimental observations usually involve the response of chemical signal with the change of applied potential, the GCP(U) can be directly used as the

function of applied potential in the quantum mechanics calculations for the electrochemical system. Given the existence of local minimum of GCP(U) in equation 3, the GCP(U) should be non-linearly related to applied potential, instead of its linear form as previous reports.[12, 13] Therefore, the $F(n)$ is at least quadratic as the function of n such that to locate the minimum of G(n, U). Next we fit $F(n)$ approximately as a quadratic form (equation 4) and minimize G(n, U) thereby resulting in GCP (U) with quadratic characteristic as formula 5.[5, 14]

$$F(n) = a(n - n_0)^2 + b(n - n_0) + c \tag{4}$$

$$\text{GCP}(U) = -\frac{1}{4a}(b - \mu_{e,\text{SHE}} + eU)^2 + c - n_0\mu_{e,\text{SHE}} + n_0 eU \tag{5}$$

These fitted parameters a, b, and c are related to the physical quantities in differential capacitance and determined from quantum mechanics calculations. According to the recent studies,[3, 15] $F(n)$ and GCP (U) can be further written as formula 6 and 7, respectively:

$$F(n) = -\frac{1}{2C_{\text{diff}}}(n - n_0)^2 + (\mu_{e,\text{SHE}} - eU_{\text{PZC}})(n - n_0) + F_0 \tag{6}$$

$$\text{GCP}(U) = \frac{e^2 C_{\text{diff}}}{2}U^2 + (en_0 - e^2 C_{\text{diff}} U_{\text{PZC}})U + F_0 + \frac{e^2 C_{\text{diff}}}{2}U_{\text{PZC}}^2 - n_0\mu_{e,\text{SHE}} \tag{7}$$

Where the variable C_{diff} and U_{PZC} are differential capacitance and potential of zero charge, respectively, while F_0 represents free energy of the neutral system ($n=n_0$, n_0 is the total valence electrons at zero net charge). They are related to parameters a, b, and c as: $C_{\text{diff}} = -\frac{1}{2a}$, $F_0 = c$, and $U_{\text{PZC}} = (\mu_{e,\text{SHE}} - b)/e$.

The quadratic form of $F(n)$ and GCP(U) reveal the non-ignorable role of capacitive

effect during the electrochemical process,[16] which is mainly due to the electron-delocalization on broad electronic band of heterogeneous catalysis system. This allows fractional occupations of electron state, i.e. the continuously varied number of electrons, which causes the capacitive contributions to electrochemical process.

Similarly, the previous studies[17, 18] also employed a quadratic form of $G(n, U)$, $G(n;U) = F(n(U)) - ne(U_{SHE} - U)$, which relies on the work function instead of thermodynamic minimization to establish the relationship between applied potential and numbers of electron. Note that the methodology used in this work does not rely on the calculation of work function and we can directly obtain the $GCP(U)$ from free energy by means of Legendre transformation. Moreover, the Legendre transformation allows us to define $F(n)$ and $GCP(U)$ with physical parameters.

The effect of number of water molecules on CO_2 reduction reaction (CO_2RR). First of all, we consider the effect of different number of explicit waters on the CO_2RR by calculating the free energy change and barrier for the system with two and four water molecules and comparing with our three-water-molecule model. It is found that all these systems present approximate change of free energy, shown in **Figure S1**, and hence we consider the current three-water-molecule-model is adequate as the representative since it balances the expensive DFT computation and the consideration of solvation effects as well as hydrogen bond net of the system.
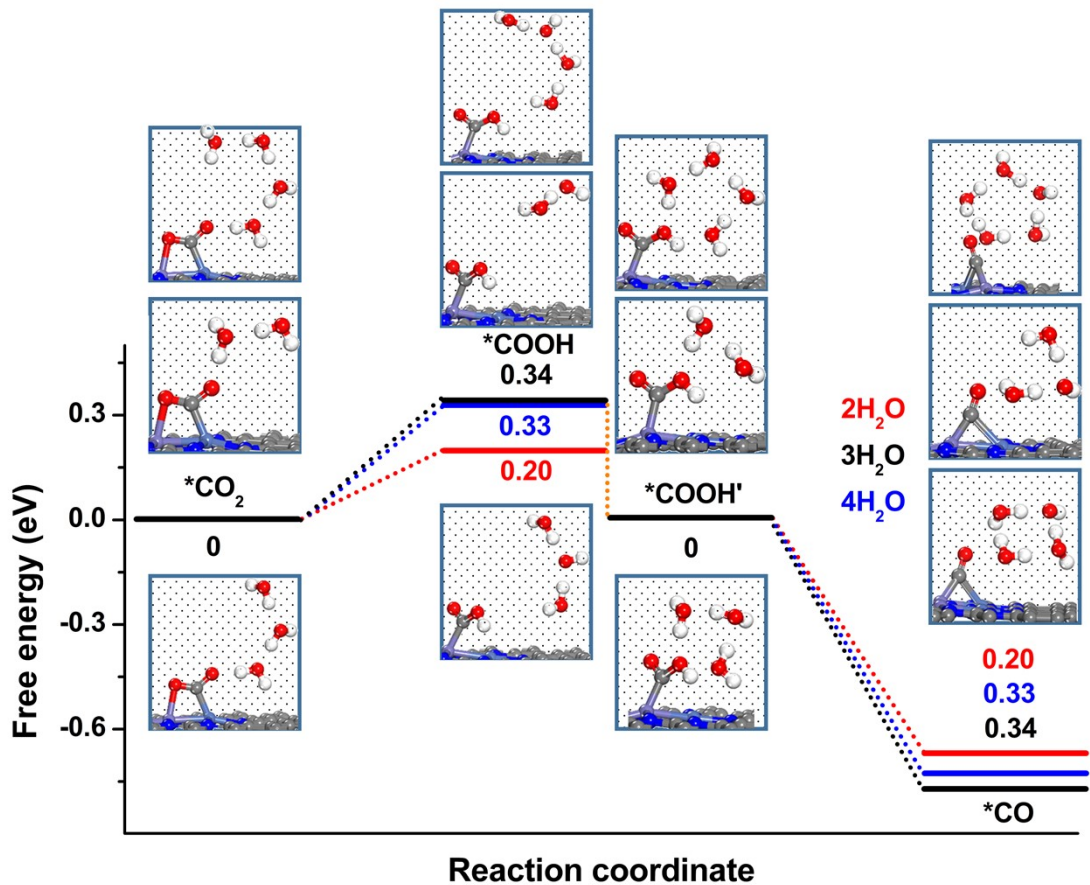
Figure S1. The $CO_2 \rightarrow CO$ converting pathway with two/three/four explicit waters to produce *COOH, *COOH', *CO, and hydroxyl ion under implicit solvation background on Fe&Ni@g-N$_6$ bi-site at the zero net electron of the system, as well as the corresponding free energy change at -0.7 V vs RHE applied potential, where the dense dots denote implicit solvation, the free energy of adsorbed CO_2 is set as zero, and the yellow dot line denotes thermodynamically spontaneous process from OH$^-$ ion to H$_2$O.
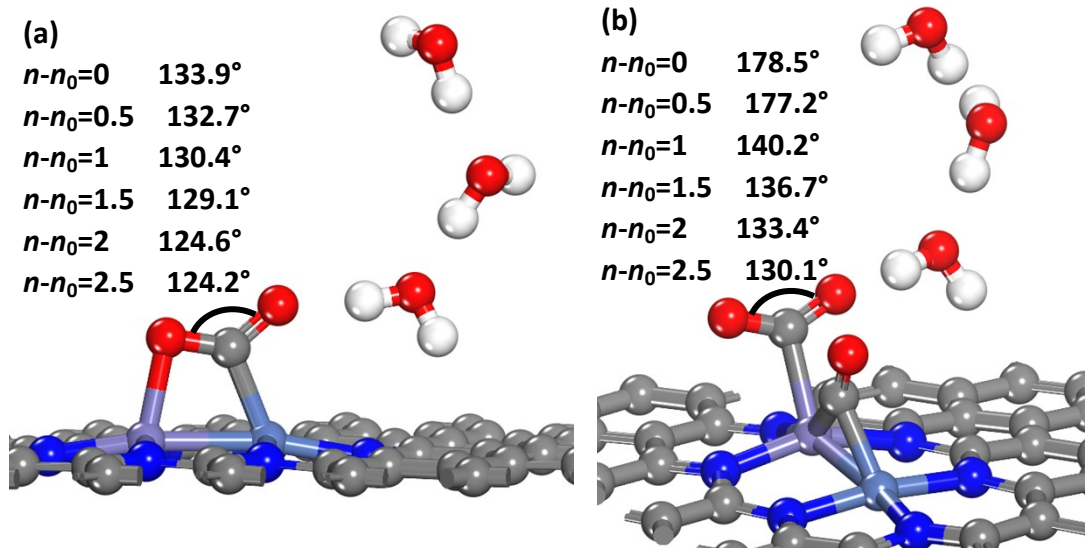
Figure S2. The O-C-O angle in CO_2 chemisorption on (a) pure Fe-Ni dimer center and on (b) *CO passivated Fe-Ni dimer center stabilized by three explicit water molecules in net charge of 0-2.5.
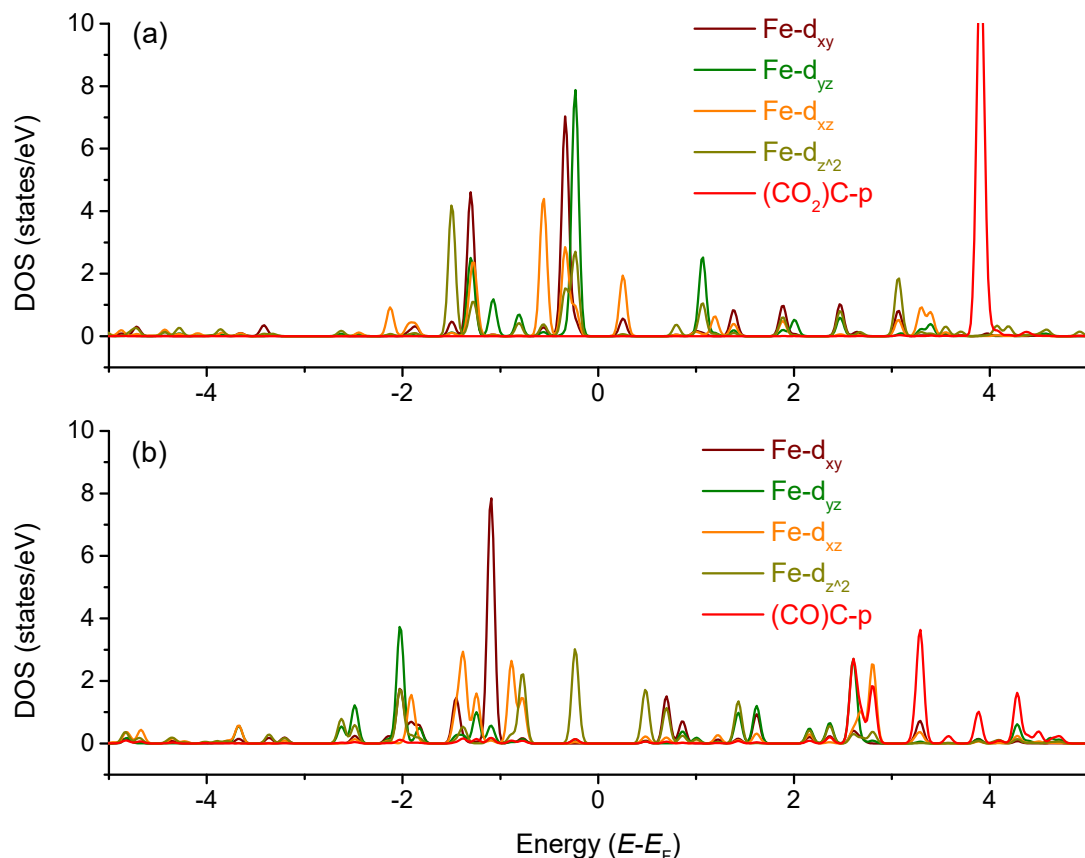
**Figure S3.** The projected density of states of p orbital of C atom of CO_2/CO adsorbed on (a) CO*Fe&Ni@g-N_6 and (b) the d orbital of Fe atom. One can see that the PDOS of d orbital of Fe

and frontier orbital of CO_2 (p orbital of C atom) shows seldom overlap in a large energy range, which reveal the weak interaction between CO_2 and Fe single site. While the PDOS of Fe (d_{yz} and d_{xz}) and CO 5σ (C-p orbital above the Fermi level, $2\pi^*$) exhibit slight overlaps, corresponding to moderate CO adsorption. These are in accordance with the adsorption free energy change for CO_2 (0.00 eV) and CO (-0.85 eV).

The comparison of VASPsol-jDFTx combination method with jDFTx potential-fixed method. Note that in our calculation procedure we did not directly apply the fixed potential optimization method as implemented in jDFTx code. This is mainly because the fixed potential method is computationally very expensive. According to the recent studies,[3,19] we can alternatively convert fixed charge free energy to fixed potential grand canonical potential by minimization of grand canonical free energies via Legendre transformation. This modified procedure needs initial VASPsol optimization and then jDFTx single point calculation, which can greatly reduce the computing time without sacrifice of the computational accuracy. To verify the reliability of this method, we take CO_2 adsorption at Fe-Ni center as the test example and optimize its structure based on the VASPsol-jDFTx combination method and jDFTx potential-fixed method. As shown in **Figure S4**, the geometric structure as well as the critical bond lengths including C=O, Fe-O, Ni-C, metal-N, and O$^{\cdots}$H bonds obtained by the two methods are very close. Particularly, the VASPsol-jDFTx method greatly reduces the computation time by seven times as compared to the more expensive potential-fixed method. This proved the rationality of the VASPsol-jDFTx method in this work.
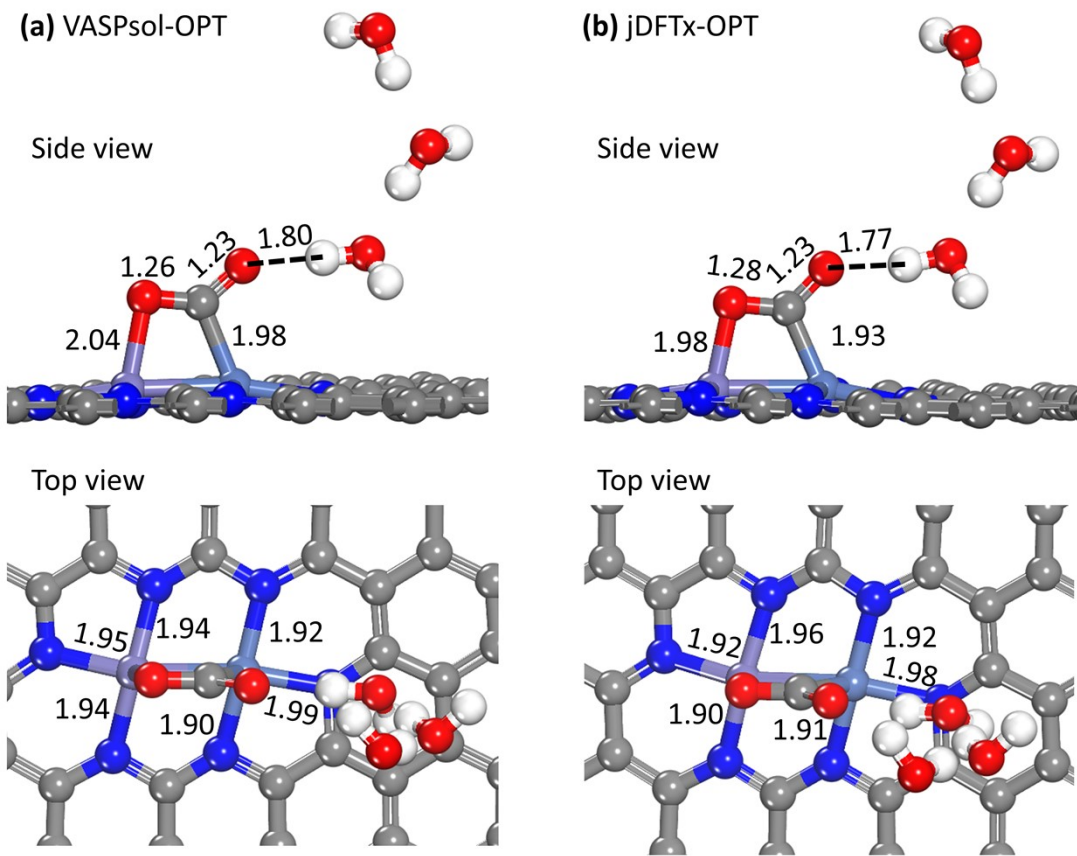
Figure S4. The optimized geometry structure and the critical bond lengths of CO_2 adsorbed on Fe-Ni bi-center by (a) VASPsol-jDFTx combination method and (b) jDFTx potential-fixed method.
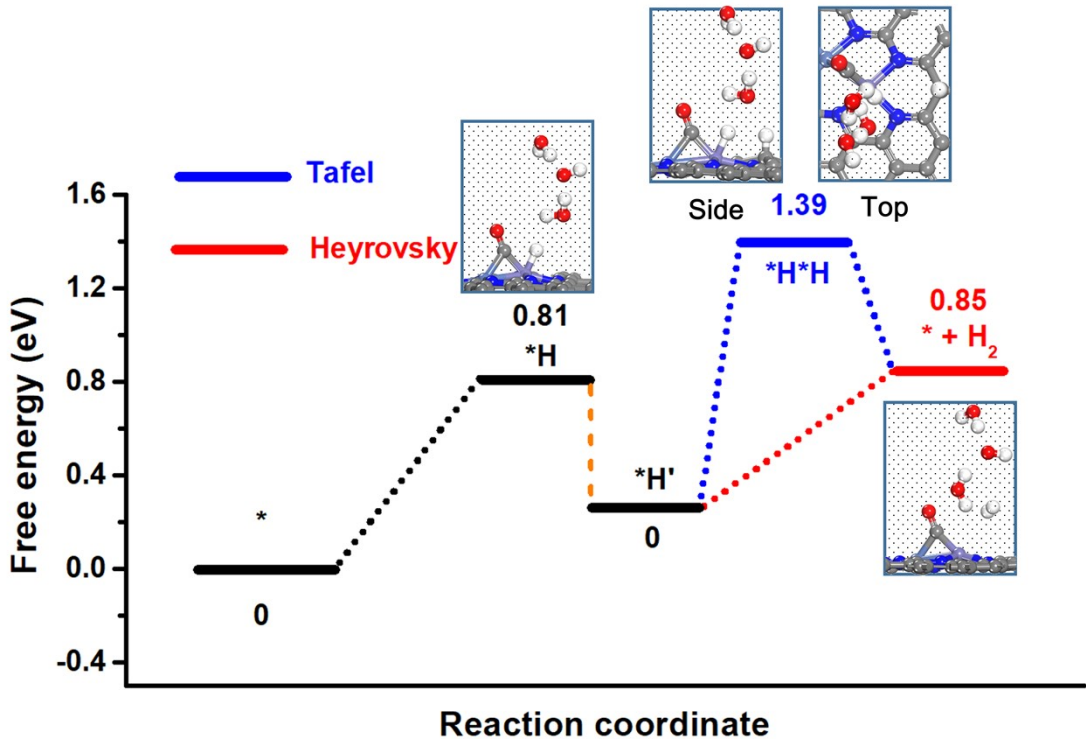
Fig. S5. Hydrogen evolution process on *CO passivated Fe-Ni dimer center at -0.7 V vs RHE and neutral electrolytic condition. The first hydrogen adsorption step or Volmer step corresponds to the free energy change of 0.81 eV. The Tafel and Heyrovsky reaction pathway need the free energy of 1.39 eV and 0.85 eV, respectively.

The data of free energy. The free energy (eV) of the stationary point and transition states along the CO_2RR pathway on Fe&Ni@g-N_6 with a series of net electron, as well as the parameters obtained from quadratic fitting of F-$n\mu_{e,SHE}$, where the * represents the Fe&Ni@g-N_6 catalyst surface while the superscript " ' " represents the corresponding explicit water state since OH^- ion is hydrogenated immediately by buffer electrolyte.

*		$n-n_0$	F	Total electron	$F-n\mu_{e,SHE}$
Parameters		0	-17290.8	232	-16209.7
a	0.28	0.5	-17292.8	232.5	-16209.3
b	0.79	1	-17294.5	233	-16208.7
c	-16209.75	1.5	-17296.0	233.5	-16207.9
		2	-17297.5	234	-16207.0
		2.5	-17298.8	234.5	-16206.1

$*CO_2$		$n-n_0$	F	Total electron	$F-n\mu_{e,SHE}$
Parameters		0	-18321.4	248	-17165.7
a	0.30	0.5	-18323.4	248.5	-17165.4
b	0.46	1	-18325.3	249	-17164.9
c	-17165.68	1.5	-18326.9	249.5	-17164.3
		2	-18328.6	250	-17163.6
		2.5	-18330.0	250.5	-17162.6

Cis-*COOH		$n-n_0$	F	Total electron	$F-n\mu_{e,SHE}$
Parameters		0	-18320.0	248	-17164.3
a	0.35	0.5	-18322.4	248.5	-17164.4
b	-0.24	1	-18325.0	249	-17164.3
c	-17164.36	1.5	-18326.6	249.5	-17163.9
		2	-18328.4	250	-17163.4
		2.5	-18330.0	250.5	-17162.8

Trans-*COOH		$n-n_0$	F	Total electron	$F-n\mu_{e,SHE}$
Parameters		0	-18319.8	248	-17164.2
a	0.39	0.5	-18322.3	248.5	-17164.2
b	-0.41	1	-18325.0	249	-17164.2
c	-17164.16	1.5	-18326.6	249.5	-17163.9
		2	-18328.4	250	-17163.4
		2.5	-18330.0	250.5	-17162.7

Cis-*COOH'		$n-n_0$	F	Total electron	$F-n\mu_{e,SHE}$
Parameters		0	-18337.5	249	-17177.2
a	0.27	0.5	-18339.5	249.5	-17176.8
b	-0.60	1	-18341.3	250	-17176.3
c	-17177.17	1.5	-18343.0	250.5	-17175.7
		2	-18344.5	251	-17174.9

		2.5	-18346.0	251.5	-17174.0

Trans-*COOH'		n-n_0	F	Total electron	F-$n\mu_{e,SHE}$
Parameters		0	-18337.4	249	-17177.0
a	0.31	0.5	-18339.4	249.5	-17176.8
b	0.48	1	-18341.3	250	-17176.3
c	-17177.07	1.5	-18343.0	250.5	-17175.6
		2	-18344.5	251	-17174.9
		2.5	-18345.9	251.5	-17174.0

*CO		n-n_0	F	Total electron	F-$n\mu_{e,SHE}$
Parameters		0	-18337.3	249	-17176.9
a	0.38	0.5	-18339.6	249.5	-17177.0
b	-0.23	1	-18341.8	250	-17176.8
c	-17176.95	1.5	-18343.8	250.5	-17176.4
		2	-18345.6	251	-17175.9
		2.5	-18347.1	251.5	-17175.2

*CO'		n-n_0	F	Total electron	F-$n\mu_{e,SHE}$
Parameters		0	-18947.1	260	-17735.5
a	0.29	0.5	-18949.0	260.5	-17735.1
b	0.67	1	-18950.8	261	-17734.6
c	-17735.89	1.5	-18952.4	261.5	-17733.8
		2	-18953.9	262	-17733.0
		2.5	-18955.3	262.5	-17732.0

*H		n-n_0	F	Total electron	F-$n\mu_{e,SHE}$
Parameters		0	-17290.1	232	-16209.0
a	0.47	0.5	-17292.5	232.5	-16209.1
b	-0.34	1	-17294.7	233	-16208.9
c	-16208.99	1.5	-17296.5	233.5	-16208.4
		2	-17298.2	234	-16207.8
		2.5	-17299.7	234.5	-16206.9

*H'		n-n_0	F	Total electron	F-$n\mu_{e,SHE}$
Parameters		0	-17307.2	233	-16221.4
a	0.29	0.5	-17309.1	233.5	-16220.9
b	0.76	1	-17310.8	234	-16220.4
c	-16221.39	1.5	-17312.4	234.5	-16219.6

		$n-n_0$	F	Total electron	$F-n\mu_{e,SHE}$
		2	-17313.8	235	-16218.7
		2.5	-17315.1	235.5	-16217.7

*H_2		$n-n_0$	F	Total electron	$F-n\mu_{e,SHE}$
Parameters		0	-17306.3	233	-16220.6
a	0.29	0.5	-17308.3	233.5	-16220.2
b	0.67	1	-17310.1	234	-16219.7
c	-16220.58	1.5	-17311.6	234.5	-16218.9
		2	-17313.1	235	-16218.0
		2.5	-17314.5	235.5	-16217.1

TS cis-*COOH		$n-n_0$	F	Total electron	$F-n\mu_{e,SHE}$
Parameters		0	-18319.4	248	-17163.7
a	0.62	0.5	-18321.8	248.5	-17163.8
b	-0.94	1	-18324.3	249	-17164.0
c	-17163.63	1.5	-18326.3	249.5	-17163.6
		2	-18328.1	250	-17163.1
		2.5	-18329.4	250.5	-17162.1

The free energy (eV) of the stationary point and transition states along the CO_2RR pathway on CO*Fe&Ni@g-N_6 passivated by *CO with a series of net electron, as well as the parameters obtained from quadratic fitting of $F-n\mu_{e,SHE}$, where the * represents the CO*Fe&Ni@g-N_6 catalyst surface while the superscript " ' " represents the corresponding explicit water state since OH^- ion is hydrogenated immediately by buffer electrolyte.

*		$n-n_0$	F	Total electron	$F-n\mu_{e,SHE}$
Parameters		0	-17884.3	242	-16756.6
a	0.31	0.5	-17886.3	242.5	-16756.2
b	0.64	1	-17888.0	243	-16755.6
c	-16756.59	1.5	-17889.7	243.5	-16754.9
		2	-17891.1	244	-16754.1
		2.5	-17892.5	244.5	-16753.1

*CO$_2$		n-n_0	F	Total electron	F-$n\mu_{e,SHE}$
Parameters		0	-18914.7	258	-17712.4
a	0.14	0.5	-18916.6	258.5	-17712.0
b	0.77	1	-18918.4	259	-17711.4
c	-17713.41	1.5	-18920.2	259.5	-17711.0
		2	-18921.9	260	-17710.3
		2.5	-18923.5	260.5	-17709.6

Cis-*COOH		n-n_0	F	Total electron	F-$n\mu_{e,SHE}$
Parameters		0	-18913.2	258	-17710.9
a	0.34	0.5	-18915.5	258.5	-17710.9
b	-0.13	1	-18918.0	259	-17710.7
c	-17710.93	1.5	-18919.6	259.5	-17710.4
		2	-18921.4	260	-17709.8
		2.5	-18923.0	260.5	-17709.1

Trans-*COOH		n-n_0	F	Total electron	F-$n\mu_{e,SHE}$
Parameters		0	-18913.0	258	-17710.7
a	0.43	0.5	-18915.5	258.5	-17710.9
b	-0.50	1	-18918.0	259	-17710.8
c	-17710.74	1.5	-18919.8	259.5	-17710.5
		2	-18921.6	260	-17710.0
		2.5	-18923.0	260.5	-17709.3

Cis-*COOH'		n-n_0	F	Total electron	F-$n\mu_{e,SHE}$
Parameters		0	-18930.7	259	-17723.7
a	0.29	0.5	-18932.6	259.5	-17723.4
b	0.64	1	-18934.4	260	-17722.8
c	-17723.74	1.5	-18936.1	260.5	-17722.1
		2	-18937.5	261	-17721.2
		2.5	-18939.0	261.5	-17720.4

Trans-*COOH'		n-n_0	F	Total electron	F-$n\mu_{e,SHE}$
Parameters		0	-18930.6	259	-17723.6
a	0.29	0.5	-18932.6	259.5	-17723.3
b	0.58	1	-18934.4	260	-17722.8
c	-17723.63	1.5	-18936.0	260.5	-17722.1
		2	-18937.5	261	-17721.3

		2.5	-18939.0	261.5	-17720.4

*CO		n-n_0	F	Total electron	F-$n\mu_{e,SHE}$
Parameters		0	-18929.5	259	-17722.5
a	0.43	0.5	-18931.8	259.5	-17722.6
b	-0.37	1	-18934.1	260	-17722.5
c	-17722.61	1.5	-18936.1	260.5	-17722.1
		2	-18937.8	261	-17721.5
		2.5	-18939.4	261.5	-17720.8

*CO'		n-n_0	F	Total electron	F-$n\mu_{e,SHE}$
Parameters		0	-18947.1	260	-17735.5
a	0.29	0.5	-18949.0	260.5	-17735.1
b	0.67	1	-18950.8	261	-17734.6
c	-17735.50	1.5	-18952.4	261.5	-17733.8
		2	-18953.9	262	-17733.0
		2.5	-18955.3	262.5	-17732.0

*H		n-n_0	F	Total electron	F-$n\mu_{e,SHE}$
Parameters		0	-17882.9	242	-16755.2
a	0.44	0.5	-17885.2	242.5	-16755.2
b	-0.35	1	-17887.5	243	-16755.1
c	-16755.16	1.5	-17889.4	243.5	-16754.7
		2	-17891.1	244	-16754.1
		2.5	-17892.6	244.5	-16753.3

*H'		n-n_0	F	Total electron	F-$n\mu_{e,SHE}$
Parameters		0	-17900.0	243	-16767.6
a	0.30	0.5	-17901.9	243.5	-16767.2
b	0.63	1	-17903.7	244	-16766.7
c	-16767.60	1.5	-17905.3	244.5	-16766.0
		2	-17906.8	245	-16765.1
		2.5	-17908.2	245.5	-16764.1

*H$_2$		n-n_0	F	Total electron	F-$n\mu_{e,SHE}$
Parameters		0	-17899.0	243	-16766.6
a	0.29	0.5	-17901.1	243.5	-16766.4
b	0.63	1	-17902.9	244	-16765.9
c	-16766.75	1.5	-17904.5	244.5	-16765.2

		$n-n_0$	F	Total electron	$F-n\mu_{e,SHE}$
		2	-17906.0	245	-16764.3
		2.5	-17907.4	245.5	-16763.4

TS cis-*COOH		$n-n_0$	F	Total electron	$F-n\mu_{e,SHE}$
Parameters		0	-18913.2	258	-17710.9
a	0.33	0.5	-18915.5	258.5	-17710.8
b	-0.08	1	-18917.6	259	-17710.7
c	-17710.91	1.5	-18919.6	259.5	-17710.3
		2	-18921.3	260	-17709.7
		2.5	-18923.0	260.5	-17709.1

TS trans-*COOH		$n-n_0$	F	Total electron	$F-n\mu_{e,SHE}$
Parameters		0	-18913.0	258	-17710.8
a	0.39	0.5	-18915.4	258.5	-17710.8
b	-0.30	1	-18917.6	259	-17710.7
c	-17710.77	1.5	-18919.6	259.5	-17710.3
		2	-18921.4	260	-17709.8
		2.5	-18923.0	260.5	-17709.1

TS cis-*CO		$n-n_0$	F	Total electron	$F-n\mu_{e,SHE}$
Parameters		0	-18929.5	259	-17722.5
a	0.32	0.5	-18931.5	259.5	-17722.3
b	0.27	1	-18933.6	260	-17722.0
c	-17722.53	1.5	-18935.3	260.5	-17721.4
		2	-18937.0	261	-17720.7
		2.5	-18938.4	261.5	-17719.8

TS trans-*CO		$n-n_0$	F	Total electron	$F-n\mu_{e,SHE}$
Parameters		0	-18929.4	259	-17722.5
a	0.37	0.5	-18931.6	259.5	-17722.3
b	0.09	1	-18933.6	260	-17722.0
c	-17722.47	1.5	-18935.4	260.5	-17721.5
		2	-18937.1	261	-17720.8
		2.5	-18938.6	261.5	-17720.0

TS *H		$n-n_0$	F	Total electron	$F-n\mu_{e,SHE}$
Parameters		0	-17883.1	242	-16755.3
a	0.44	0.5	-17885.4	242.5	-16755.3

b	-0.07	1	-17887.4	243	-16755.0
c	-16755.36	1.5	-17889.1	243.5	-16754.4
		2	-17890.8	244	-16753.7
		2.5	-17892.1	244.5	-16752.8

The contribution of vibrational entropy involving zero-point energy (ZPE), vibrational enthalpy (H_{vib}), and vibrational entropy ($-TS_{vib}$) to free energy of the stationary point and transition states along the CO_2RR pathways on pure Fe&Ni@g-N_6 and*CO passivated CO*Fe&Ni@g-N_6, where the * represents the adsorption on catalyst surface.

Fe&Ni@g-N_6	eV	CO*Fe&Ni@g-N_6	eV
*CO_2	2.01	*CO_2	2.17
Cis-*COOH	1.96	Cis-*COOH	2.07
Trans-*COOH	1.91	Trans-*COOH	2.01
*CO	2.13	*CO	2.27
*H	2.09	*H	2.12
*H_2	1.94	*H_2	1.96
TS cis-*COOH	1.97	TS cis-*COOH	2.07
TS trans-*COOH	1.91	TS trans-*COOH	2.01
TS cis-*CO	2.13	TS cis-*CO	2.20
TS trans-*CO	2.22	TS trans-*CO	2.32
TS *H	2.10	TS *H	2.14

Table S1. The fitting parameter a and the corresponding capacitance of the electrochemical system with different adsorption species, where the capacitance is related to the parameter "a" as $C_{diff} = -\dfrac{1}{2a}$, and it can be converted to the unit of $\mu F\ cm^{-2}$.

Fe&Ni@g-N_6	a	C_{diff} ($\mu F\ cm^{-2}$)	CO*Fe&Ni@g-N_6	a	C_{diff} ($\mu F\ cm^{-2}$)
*	0.28	21.81	*	0.31	19.70
*CO_2	0.30	20.36	*CO_2	0.14	43.62
Cis-*COOH	0.35	17.45	Cis-*COOH	0.34	17.96
Trans-*COOH	0.39	15.66	Trans-*COOH	0.43	14.20

Cis-*COOH'	0.27	22.62	Cis-*COOH'	0.29	21.06
Trans-*COOH'	0.31	19.70	Trans-*COOH'	0.29	21.06
*CO	0.38	16.07	*CO	0.43	14.20
*CO'	0.29	21.06	*CO'	0.29	21.06
*H	0.47	12.99	*H	0.44	13.88
*H'	0.29	21.06	*H'	0.30	20.36
$*H_2$	0.29	21.06	$*H_2$	0.29	21.06
TS cis-*COOH	0.62	9.85	TS cis-*COOH	0.33	18.51
			TS trans-*COOH	0.39	15.66
			TS cis-*CO	0.32	19.08
			TS trans-*CO	0.37	16.51
			TS *H	0.44	13.88

Kinetics calculation. In this work, we carry out the overall kinetics calculation of CO_2RR relying on micro-kinetic model, herein the Eyring rate equation is written as:

$$k_{ij}(U) = \frac{k_B T}{h} \exp(\frac{-\Delta G_{ij}^{\ddagger}(U)}{k_B T})$$

And the rate equations for all species are defined as:

$$\frac{dx_0}{dt} = -(k_{01}+k_{02}+k_{04})x_0 + k_{10}x_1 + k_{20}x_2 + k_{30}x_3 + (k_{40}+k'_{40})x_4$$

$$\frac{dx_1}{dt} = k_{01}x_0 - (k_{10}+k_{13})x_1 + k_{31}x_3$$

$$\frac{dx_2}{dt} = k_{02}x_0 - (k_{20}+k_{23})x_2 + k_{32}x_3$$

$$\frac{dx_3}{dt} = k_{13}x_1 + k_{23}x_2 - (k_{31}+k_{32}+k_{30})x_3$$

$$\frac{dx_4}{dt} = k_{04}x_0 - (k_{40}+k'_{40})x_4$$

, where x_i represents the concentration of each intermediate species, $\Sigma_i x_i = 1$, while $k_{ij}(U)$ denotes the potential dependent rate constant. The subscript of adsorption species 0, 1, 2, 3, and 4 stands for $*CO_2$, cis-*COOH, trans-*COOH, *CO, and *H, respectively. Since we mainly focus on the steady state electrochemical process, the

left-hand sides of the above differential equations can be set to zero. Then the corresponding rate constants and the concentrations can be obtained by solving the equation set. Based on the calculated rate constants and the concentrations of each species, we can obtain the potential determined current density, j (mA cm^{-2}), and turnover frequency (TOF) according to the following formula: $j = a\, n\, F\, x_{CO}\, k_{CO}\, \rho_{Fe-Ni}$; $TOF = J\, t\, FE_{CO}/(n\, F\, \rho_{Fe-Ni})$, where a represents the ratio of metal load between experiment and theory (a = 1.31% (exp.) /16.9% ((59×1+55.8×1)/(40×12+6×14+59×1+55.8×1)) = 0.0775), n is the number of transferred electrons (here n = 2), F is Faraday constants, x_{CO} is the concentration of *CO at the applied potential, k_{CO} is the rate constants, ρ_{Fe-Ni} is the Fe-Ni active sites density (N_{site}/S = 1/(12.3386×12.3386×sin120°) = 7.58 × 10^{13} sites/cm^2), J is the average current in a period t of electrocatalysis, and FE_{CO} (Q_{CO}/Q_{total}) is the Faradays efficiency. In this work, we consider only two possible products, CO and H$_2$, thus the number of electrons required to generate them are the same (n = 2), and FE_{CO} can be approximated to be x_{CO}.

References

1. C. D. Taylor, S. A. Wasileski, J. S. Filhol and M. Neurock, *Phys. Rev. B: Condens. Matter Mater. Phys.*, 2006, **73**, 165402.

2. C. D. Taylor and M. Neurock, *Curr. Opin. Solid State Mate. Sci.*, 2005, **9**, 49-65.

3. Y. F. Huang, R. J. Nielsen and W. A. Goddard, *J. Am. Chem. Soc.*, 2018, **140**, 16773-16782.

4. C. D. Taylor and M. Neurock, *Curr. Opin. Solid State Mater. Sci.*, 2005, **9**, 49-65.

5. C. D. Taylor, S. A. Wasileski, J. S. Filhol and M. Neurock, *Phys. Rev. B*, 2006, **73**, 165402.

6. D. Kim, J. J. Shi and Y. Y. Liu, *J. Am. Chem. Soc.*, 2018, **140**, 9127-9131.

7. E. Skulason, G. S. Karlberg, J. Rossmeisl, T. Bligaard, J. Greeley, H. Jonsson and J. K. Norskov, *Phys. Chem. Chem. Phys.*, 2007, **9**, 3241-3250.

8. Y. Sha, T. H. Yu, B. V. Merinov and W. A. Goddard, *J. Phys. Chem. C*, 2012, **116**, 6166-6173.

9. R. Jinnouchi and A. B. Anderson, *Phys. Rev. B*, 2008, **77**, 245417.

10. R. Sundararaman and W. A. Goddard, *J. Chem. Phys.*, 2015, **142**, 064107.

11. J. D. Goodpaster, A. T. Bell and M. Head-Gordon, *J. Phys. Chem. Lett.*, 2016, **7**, 1471-1477.

12. H. Xiao, T. Cheng, W. A. Goddard and R. Sundararaman, *J. Am. Chem. Soc.*, 2016, **138**, 483-486.

13. K. Chant and J. K. Norskov, *J. Phys. Chem. Lett.*, 2016, **7**, 1686-1690.

14. M. Mamatkulov and J. S. Filhol, *Phys. Chem. Chem. Phys.*, 2011, **13**, 7675-7684.

15. R. Sundararaman, K. Letchworth-Weaver, K. A. Schwarz, D. Gunceler, Y. Ozhabes and T. A. Arias, *SoftwareX*, 2017, **6**, 278-284.

16. K. R. Chan and J. K. Norskov, *J. Phys. Chem. Lett.*, 2015, **6**, 2663-2668.

17. M. J. Janik, C. D. Taylor and M. Neurock, *J. Electrochem. Soc.*, 2009, **156**, B126-B135.

18. X. H. Zhao and Y. Y. Liu, *J. Am. Chem. Soc.*, 2020, **142**, 5773-5777.

19. M.D. Hossain, Y.F. Huang, T.H. Yu, W.A. Goddard and Z.T Luo, *Nat. Commun.* 2020, **11**, *2256*.